

Channel Impulse Response Measurement for Characterizing The Ionosphere Communication Channel Over Java Island Indonesia

Varuliantor Dear^{1,2}, Iskandar¹, Prayitno Abadi³, Cahyo Purnomo⁴, Asnawi
Husin², and Adit Kurniawan¹

¹Sekolah Teknik Elektro dan Informatika - Institut Teknologi Bandung

²Pusat Riset Antariksa - Badan Riset dan Inovasi Nasional

³Pusat Riset Iklim dan Atmosfer - Badan Riset dan Inovasi Nasional

⁴Stasiun Observasi Antariksa Atmosfer Sumedang - Badan Riset dan Inovasi Nasional

¹Jl. Ganesa 20 Lebak Siliwangi, Bandung, Indonesia

²Jl. Cisitua Sangkuriang, Bandung, Indonesia

³Jl. Jl. Cisitua Sangkuriang, Bandung, Indonesia

⁴Jl. Jl. Raya Bandung-Sumedang, Sumedang, Indonesia

Key Points:

- Development of ionosphere channel impulse response measurement system to obtained the empirical data of Delay Spread and Doppler Spread
- The system is placed over Java island Indonesia which part of Low-Latitude-Equatorial Ionosphere Anomaly region
- The system is ready to be used for collecting further data in order to characterize the ionospheric communication channel comprehensively

Abstract

For designing a digital High Frequency (HF) radio communication system in the sky-wave propagation mode, Delay spread and Doppler spread are the fundamental parameters of ionosphere channel characteristics that need to be known. Although the International Telecommunication Union (ITU) already provides general classification values for three different regions and conditions as a recommendation, the empirical Delay spread and Doppler spread values are still needed for an optimum design. As the role of HF communication in Indonesia is still important and its development technology is continued, the empirical data of ionosphere channel characteristics are also needed. However, the comprehensive empirical data of ionosphere channel characteristics over Indonesia is difficult to find. In this research, we developed an Ionosphere Channel Impulse Response (CIR) measurement system based on Software Defined Radio (SDR) with purpose to obtain the empirical values of Delay spread and Doppler spread. The measurement system is placed in Java Island Indonesia, which is in the Low latitude - Equatorial Ionosphere Anomaly (EIA) region. The specification of the system was determined based on the increased values of ITU parameters for low-latitude regions in order to be able to capture the possibility of higher values. The early measurement result shows slightly different values from ITU recommendation which is probably due to the EIA regions effect. This system is ready to collect further data to characterize the ionospheric communication channel comprehensively and investigate the space weather impact on HF communication systems.

Plain Language Summary

Delay spread and Doppler spread are the fundamental parameter of a communication channel that should be known for designing the wireless digital communication system. Those parameters should also be known for designing the High Frequency (HF) digital communication system. Although International Telecommunication Union (ITU) already provides general values for three different locations and conditions, the empirical values of Delay spread and Doppler spread still need to be known for an optimum design. In this research, we reported the development of the ionospheric channel impulse response measurement system over Java Island Indonesia which is part of the low-latitude - Equatorial Ionosphere Anomaly (EIA) region. The purpose of the measurement system is to obtain the empirical Delay spread and Doppler Spread values with the specification of the system based on the increased values of ITU recommendation in order to be able to capture the possibility of higher values that could be occurred in the EIA region. Early measurement results show slightly different values from ITU recommendation which is probably due to the EIA region effect. This system is ready to use for collecting more data for characterizing the ionosphere communication channel comprehensively and for investigating the space weather impact on HF communication systems

1 Introduction

Ionosphere is one of the radio wave propagation mediums provided by nature for Beyond Line of Sight (BLOS) propagation in the High Frequency (HF) radio spectrum. Based on the advantages of the BLOS propagation, which are: (i) long-distance coverage area, (ii) minimum infrastructure requirement, and (iii) relatively low cost (Maslin, 1988), HF radio communication is used widely for military communication (Eliardsson et al., 2015) (Withington, 2020), post-disaster communication (Kitano et al., 2006), and regular communication with remote areas (Porte et al., 2018) (Abdullah et al., 2018). Those advantages are the basic reasons for the continuous development of HF Radio communication systems which transform into digital communication systems (Wang et al., 2018). However, for the development of an optimum digital communication systems, the fundamental information that should be known is the channel characteristic in terms of

Delay Spread and Doppler Spread parameters (Andersen et al, 1995). The Delay spread is the spreading of the arrival time of radio wave multipath components through a channel, and the Doppler Spread is the spreading of the received frequency through the channel. Regarding to this important consideration, the characteristic of ionosphere channel should also be known for the design of HF digital communication system.

As part of space weather components, Ionosphere known as a dispersive communication channel which have temporal and spatial variations (Goodman, 2005). For general reference in the design and test of HF digital modems, International Telecommunication Union (ITU) already provides the ionospheric channel characteristic parameters values as a recommendation (ITU, 2000). ITU generally classified the ionosphere channel into three different regions and conditions for Delay spread and Doppler spread channel parameters. The classification of three different regions of ITU are low latitude, middle latitude, and high latitude. Meanwhile, the classification of three conditions of the ionosphere are quiet, moderate, and disturbed. Those recommendation values are helpful for basic digital communication design. However, some research shows that the empirical data of channel characteristics are still needed in order to achieve the optimum design for real world implementation (Ads et al., 2015) (Bergada et al., 2014) (Angling et al., 1998). Therefore, for the development of HF digital communication in Indonesia, the empirical data should also available. From the perspective of ionospheric physic mechanism, Indonesia is part of low latitude regions with some islands are rely on the Equatorial Ionospheric Anomaly (EIA) region. The Ionosphere in EIA regions known to have higher electron density from other low-latitude regions due to the "fountain effect" mechanism (Duncan, 1960) and also a concentration of ionosphere scintillation. Therefore, empirical data of ionosphere channel characteristics over Indonesia will also contribute to the knowledge of the ionosphere behaviours in the low latitude-EIA regions as part of space weather dissemination.

The Delay Spread and Doppler Spread could be obtained from the Channel Impulse Response (CIR) measurement (Salous, 2013). To the best of our knowledge, the research for measuring the channel impulse response in Indonesia is difficult to found, except that has been done by Kurniawati et al.(2018). They investigated the statistical channel model of the ionosphere for 3044 km link between Surabaya and Merauke from 5 days of measurement. Their research shows the distribution of Delay spread with mean values in the range of 0–100 ms, 100–500 ms, and 500–1300 ms for 3 cluster multi-hop modes namely 2F, 3F, and 4F. Those values are significantly higher compared to the ITU recommendation. From our perspective, those higher values probably are not defining the "pure" of ionosphere communication channel characteristics due to the factor of earth-surface reflections in the long haul multi-hop propagation mode. Therefore, these results could not be suitable to be used for characterizing the basic ionosphere channel behaviours. Besides the possibility of influencing factors from the earth's surface reflection, the relative-short period of measurement are not enough to be use for three classification ionosphere conditions as given by ITU. For characterizing the ionosphere channel, this research could be improved by using different geometry of transmitter and receiver location alongside with its period of measurement. In this research, we develop the ionosphere channel impulse response measurement system for low latitude region and in Near Vertical Incidence Skywave (NVIS) propagation mode in order to obtain the empirical Delay Spread and Doppler spread values for characterizing the ionosphere communication channel. The development of the system is based on the Software Defined Radio (SDR) platform and placed in Java island Indonesia which is rely on the crest region of Low Latitude-Equatorial Ionosphere Anomaly (EIA). To have a comprehensive report, the structure of this paper is written as follows: in section 2 brief theory of channel impulse response measurement is described. In section 3, the design of the measurement method and the determination of system parameters including the data post-processing is described. In section 4 Result from operational testing and its discussion are described. In the last section, the conclusion of this paper are given.

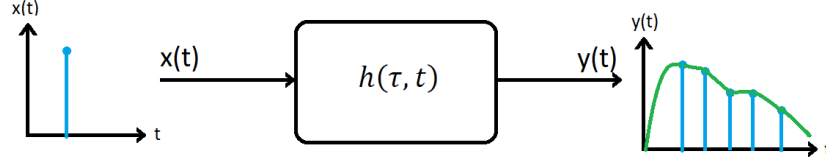


Figure 1. Linear time variant system model as representation of multipath channel.

2 Channel Impulse Response Measurement

A multipath wireless channel could be represented as the Linear Time-Variant model and could be characterized by its Channel Impulse Response (CIR) as illustrated in Figure 1. The output of model $y(t)$ is the convolution of input $x(t)$ with the channel impulse response $h(t, \tau)$. From the channel impulse response, the information of multipath of radio wave propagations in the channel could be known in terms of its arrival time and its phase. For the ionosphere, the channel impulse response measurement could also be used for characterizations which needed in the design of digital communication system. The channel impulse response in the discrete form could be written as follows:

$$h(t, \tau) = \sum_{n=1}^N \alpha_n(t) e^{(-j\varphi_n(t))} \delta(\tau - \tau_n(t)) \quad (1)$$

where α_n is the path loss and shadowing function, φ_n as the phase and Doppler function, and δ is direct function for N number of multipath components. From $h(t, \tau)$, the scattering function $S(f, \tau)$ of a channel could be calculated using equation as follows:

$$S(f, \tau) = \int_{-\infty}^{\infty} R_{hh}(\Delta t, \tau) e^{(-j2\pi f \Delta t)} \partial \Delta t \quad (2)$$

where R_{hh} is the autocorrelation function of $h(t, \tau)$. The Scattering function $S(f, \tau)$ consists of two variable channels which are Power Delay Profile (PDP) and Doppler Spectrum. Power Delay Profile is a function of time that describe the spreading of the time delay of the channel and could be expressed in equation as follows:

$$P(\tau) = \int_{-\infty}^{\infty} S(f, \tau) \partial f \quad (3)$$

For the spreading of frequency or Doppler spectrum, the calculation could done using equation as follows:

$$P(f) = \int_{-\infty}^{\infty} S(f, \tau) \partial \tau \quad (4)$$

From the spreading of the time delay or Delay spread and the spreading of Doppler frequency or Doppler spread, the Bandwidth coherence and the Time coherence of channel could be obtained, respectively (Goldsmith, 2005). Bandwidth coherence and Time coherence are useful for determining the digital communication system parameters for an optimization.

3 Methodology

3.1 System Design

One of the popular techniques to measure the channel impulse response is a correlator channel sounder where firstly introduced by (Cox, 1975). In correlator channel sounder, an impulse signal which is represented by the Pseudo Random Bit Sequence

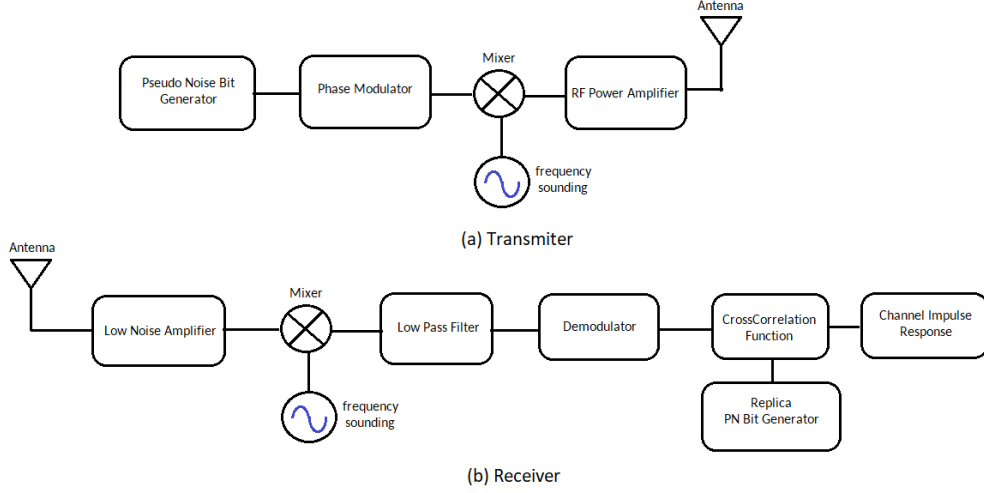


Figure 2. Correlator channel sounder block diagram for measuring the Ionospheric Channel Impulse Response.

(PRBS) is send to the measured channel in order to be analyzed using its autocorrelation function on the receiver side. From the autocorrelation result, the number of generated impulses in the channel could be obtained which represents the number of multipath propagations in the channel. To avoid the mistaken calculation, the PRBS should have a good autocorrelation property. There are some PRBS that could be selected such as Maximum Length Sequence, Barker code, Gold code, and Kasami code (Salous, 2013).

The block diagram of the correlator channel sounder for measuring the Ionosphere channel impulse response is shown in Figure 2. The transmitter block consists of Pseudo Noise (PN) code generator, Phase Modulator, Mixer, Radio Frequency Power Amplifier (RFP), and Antenna. The PN code generator block generates the Pseudo Random Bit Sequence. In this study, the Maximum Length Sequence (MLS) bit was chosen. The PN bit sequence is then phase-modulated by the phase modulator block. The signal from the output of the modulator block is shifted from baseband frequency to the selected pass-band frequency in the mixer block. The magnitude of the signal output from the mixer block is increased in the RFP block before being transmitted to the air by the antenna.

On the receiver side, the block diagram consists of Antenna, Low Noise Amplifier (LNA), Mixer, Low Pass Filter (LPF), Demodulator, and Cross-Correlation function together with replica of the transmitted PN Bit Generator as part of the signal processing block. The magnitude of the received signal from the antenna is increased in the LNA block and then down-shifted to the baseband frequency by Mixer and Low Pass Filter block. The signal output from the Low Pass Filter block is then demodulated in the Demodulator block and continued to be processed in the cross-correlation function block using the replica of the transmitter PN bit sequences. The output of cross correlation function block is the channel impulse response which used to analyze the ionosphere channel characteristics.

3.2 Determination of Software Defined Radio Parameters

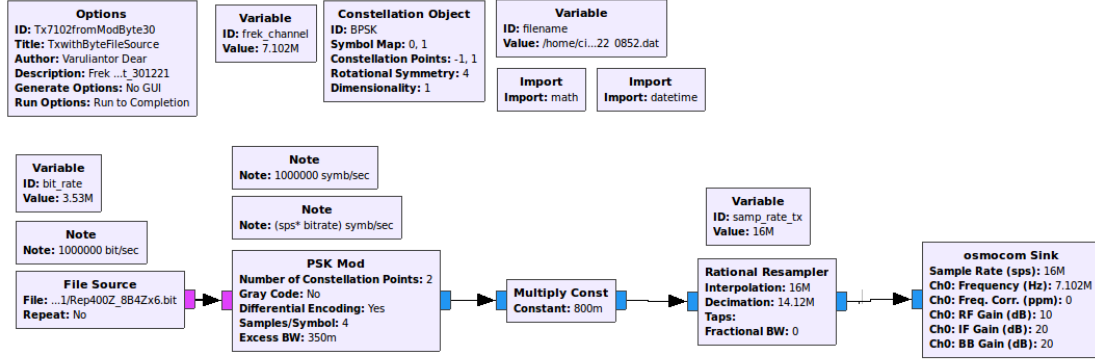
The temporal and spatial variation of the ionosphere are needed to be considered when determining the specification of the Ionosphere CIR measurement system. For mea-

183 suring the ionosphere channel characteristic over Java Island, Indonesia, the basic spec-
 184 ification of CIR measurement system could be chosen from ITU recommendation doc-
 185 ument for low latitude region as the minimum values. Those values are increased with
 186 the consideration that Java Island is part of the crest region of Equatorial Ionosphere
 187 Anomaly (EIA), which probably have higher values. The specification parameters of the
 188 ionosphere CIR measurement system are Time delay resolution (τ_{res}), Delay maximum
 189 (τ_{max}), and Maximum Doppler Frequency (fD_{max}). For this ionosphere CIR measure-
 190 ment system, the resolution of time delay is selected to be 5 times higher than the de-
 191 lay spread values from ITU recommendation for low latitude region in normal condition.
 192 The selected value was based on the consideration of the possibility of faster arrival time
 193 between each propagation path in the ionosphere. For the maximum of the time delay,
 194 the selected value is also 5 times higher than ITU Delay spread recommendation for low-
 195 latitude region with disturbed condition. The consideration of these selected values was
 196 from the possibility of the larger number of multi-hop radio wave propagation due to the
 197 occurrence of Equatorial Spread-F (ESF) which makes the ionosphere layer is in unsta-
 198 ble conditions (Abdu, 2001). For the Doppler frequency maximum, the selected value
 199 was 2 times higher than the value of Doppler Spread that given by ITU in low latitude
 200 region with disturbed condition. The Doppler frequency value could be increased more
 201 by using the sliding correlator technique in the post processing stage (Pirkl and Durgin,
 202 2008). Those specification parameters value will determine the parameter value of cor-
 203 relator channel sounder that used for this CIR measurement system design. In Table 1,
 204 the relation between target value for specification of ionosphere CIR measurement sys-
 205 tem with the ITU recommendation values are presented.

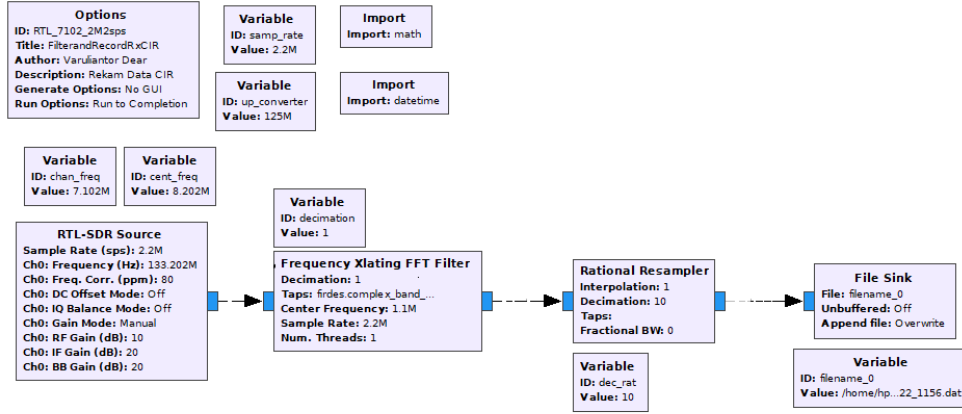
Table 1. Determination of ionosphere CIR specification target

| Parameter | ITU Rec F.1487 Value | Target Value | Remark |
|---|-------------------------|-----------------|---|
| Time delay resolution (τ_{res}) | 0.5 ms | 0.1 ms | Delay Spread for low latitude with Quiet Condition |
| Max time delay (τ_{max}) | 6 ms | 30 ms | Delay Spread for low latitude with Disturb Condition |
| Max Doppler frequency(fD_{max}) | 10 Hz | >10 Hz | Doppler Spread for low latitude with Disturb Condition |

206 For optimum practical implementation, the determination of channel sounder pa-
 207 rameter values could use algorithm that provided by (Pirkl and Durgin, 2008). In this
 208 observation system, we determine the SDR parameters that will be used for the contin-
 209 uous operational system. The GNU Radio block diagram that used for implementing the
 210 correlator channel sounder is shown in Figure 3. In the transmitter side, file source block
 211 is used to read the prepared file which consists of PN bit sequence. The PN bit sequence
 212 from file source block are modulated by the Phase Shift Key (PSK) modulation block
 213 and resulting the modulated signal in the baseband spectrum. This modulated signal
 214 is re-sampled in the block rational resampler to meet the required sampling rate of Os-
 215 mocom sink block that used for shifting the signal to the selected sounding frequency
 216 while maintaining the bit rate. The Osmocom sink block is related with the specifica-
 217 tion of SDR hardware that used for transmitting the signal over the air. In this study
 218 HackRF one is used for the transmitter SDR hardware with sampling rate up to 20 Mega
 219 Symbols per Second (MSps) and frequency range 100 kHz to 6 GHz (Ossmann, 2016).
 220 From the configuration block diagram in GNU Radio and using an assumption that for



(a) Transmitter



(b) Receiver

Figure 3. Implementation of Correlator Channel Sounder in the GNU Radio software

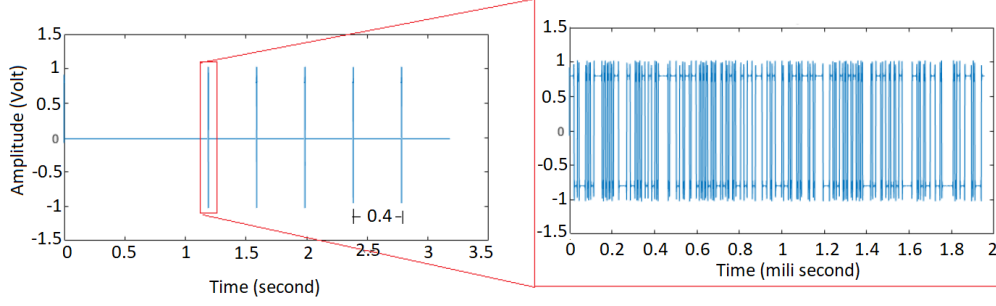


Figure 4. Waveform of sounding signal

one transmission is only consists of a single chip waveform, the determination of sampling rate values to meet the specification target in Table 1 could be use equation $Samplingrate = sps.bitrate$ where sps is the number of sample per symbol in modulator block diagram and bit rate is the number of bit that should be transmitted in one second which is equal to f_{chip} value. The modulation that use is Binary Phase Shift Keying (BPSK). Therefore, the values of sps is 2 which resulting the minimum of sampling rate is 20000 sample per symbol. This value is below the specification of the SDR hardware and potentially could be implemented. Regarding to the target of time delay maximum and chip rate value, the bit PN sequence length could be determined using equation as follows:

$$L = \tau_{max} f_{chip} = \frac{\tau_{max}}{\tau_{res}} \quad (5)$$

which resulting the length of PN bit sequence is 300. However, as the generation of Maximum Length Sequence bit is in the form of shift register where the length value is based on powers of 2, the closest value is 255 which resulted from 2^8 . This selection of L will result τ_{max} is 25.5 ms. Although this value is different from the targeted delay maximum specification value, this value still higher compared to the ITU recommendation and could be accepted for the design of the ionosphere CIR measurement system.

The use of bit PN sequence with length 255 as the waveform for single sounding signal is already met with the specification target of CIR System. However, based on the consideration to the many possibilities of interference in the HF spectrum (Chen et al., 2010), the modification of sounding signal should be done with purpose to anticipate the interferences. Therefore, the sounding signal were modified by reshaping the waveform into 5 cluster of PN bit sequence with different time from each nearest neighbour of cluster PN bit is set to 0.4 second as shown in Figure 4. Beside for the redundancy purpose, the modification also intended for easier detection in the receiver side as the waveform contains more energy (Bole et al., 2014). This signal sounding modification is not changing the chip rate value of the system.

For the implementation of the receiver block in the GNU Radio, the block diagram is simpler than the transmitter as it is intended for the post-processing technique. The block diagram are consist of RTL-SDR, Frequency Xlating FFT Filter, Rational Resampler, and File Sink Block. RTL-SDR and Frequency Xlating FFT Filter block are used for capture the passband signal and shifted to the baseband forms. The baseband signal then resampler using rational resampler block to reduce the bandwidth of received signal up to 220 kHz which inherently reduced the size of the received signal without losing any information that needed for CIR calculation. At the File Sink block, the received signal were recorded for post-processing stage. The parameters of RTL SDR Block are related to the parameter of SDR hardware device which are sampling rate and frequency. In this study, the RTL-SDR hardware with chipset RTL2832U is used. The frequency

range and sampling rate maximum of RTL-SDR hardware is 50 MHz to 1,8 GHz and 3,2 Msps, respectively (Laufer, 2014). Based on RTL-SDR device specification, the RTL-SDR could not capture the signal in the High Frequency spectrum. Therefore, the RTL SDR should be companion with Ham-It-Up Converter device which have function for direct sampling process. The combination with Ham-It-Up make RTL-SDR hardware able to capture the signal below 30 MHz (Drongowski, 2020). With this configuration, the value of frequency in the RTL-SDR block should also modified by adding the selected of sound-ing frequency with 125 MHz. The parameter values of GNU radio and its relation to achieved specification of CIR system are shown in Table 2.

Table 2. GNU Radio parameter values and achieved specification of CIR measurement system

| Parameter | Value |
|--------------|--------------|
| f_{chip} | 10000 bps |
| L_{PN} | 255 bit |
| $Samp\ rate$ | 20000 symb/s |
| sps | 2 |
| τ_{res} | 0.196 ms |
| τ_{max} | 25.5 ms |
| fD_{max} | 19.6 Hz |

3.3 Additional Consideration for System Development

To measure the ionosphere channel impulse response, the radio wave propagation from transmitter antenna to the receiver antenna should be only in the skywave propagation mode. There are some variations of sky wave propagation mode which could be seen from the number of radio wave propagation hop between earth surface and ionosphere (Davies, 1965). One of the main factors for sky wave propagation mode is the geometry of the transmitter-receiver location which is related to the earth curve. The simplest geometry of skywave propagation mode is Near Vertical Incidence Skywave (NVIS) where the dominant number of the skywave radiowave propagation is the single hop which illustrated in Figure 5. The coverage distance area of NVIS mode is less than 200 km which relatively short for ground wave propagation mode (Murugan et al., 2008). Therefore, to guarantee the CIR measurement is only in the form of NVIS propagation and not in the ground wave propagation, the consideration for implementations are follows:

3.3.1 Determination of Transmitter and Receiver Locations

The transmitter and receiver locations for the CIR measurement are Pameungpeuk West Java (7.65S, 107.69E) and Bandung West Java (6.89 S, 107.59 E), respectively. The selection of those locations was firstly based on the available location and resources for long duration and continuous measurement purpose. The HF radio wave propagation between Pameungpeuk and Bandung already analyzed by (Jiyo, 2010) which conclude that the propagation of HF radio wave is only in the skywave propagation. The considerations of transmitter and receiver locations was also based on the availability of ionosonde instrument in Pameungpeuk which could provide the ionosphere density profile for confirmation and validation of the ionosphere conditions for this research. The map of transmitter and receiver locations are shown in Figure 6. The terrain between Bandung and Pameungpeuk is an east-west mountain chains which naturally blocking the ground wave propagation mode.

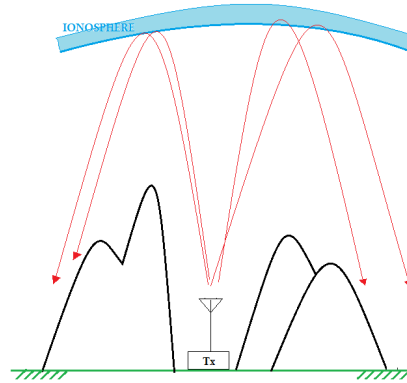


Figure 5. Illustration of Near Vertical Incident Skywave (NVIS) propagation mode

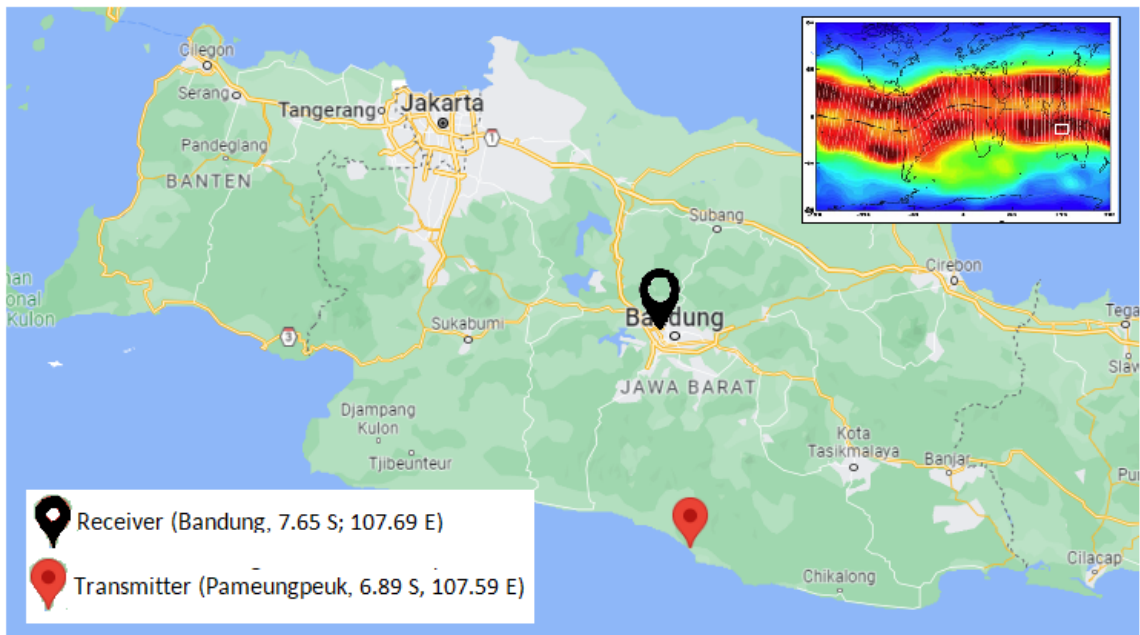


Figure 6. Location of Transmitter and Receiver Station

3.3.2 Selection of Sounding Frequency

The variation of ionosphere plasma density is affecting the frequency of radio wave that could be “reflected” to the earth’s surface. Therefore, to overcome this condition, the selection of the sounding frequency could be based on the frequency management method that usually use in HF radio communication plans (Maslin, 2017). In the frequency management method, the frequency was selected based on the variation of critical frequency of F layer (foF2) and minimum frequency (fmin) parameters from the ionosphere model. The frequency with the highest probability to appear between the foF2 and fmin values in the period of communication time is selected in order to guarantee the success of communication. In this study, the selection of the sounding frequency for CIR measurement is using Frequency management method based on the ionosphere model from Ionosphere Prediction System (IPS) Australia, namely Advance Stand Alone Prediction System (ASAPS) software (Commonwealth of Australia, Bureau of Meteorology, 2022). Model of foF2 and fmin were calculated for Bandung-Pameungpeuk circuits where its result shown in Figure 7. The models output from ASAPs are the Maximum Usable Frequency (MUF) and Absorption Lowest Frequency (ALF) which representing the foF2 and fmin values, respectively. From the model results, sounding frequency that selected in the CIR measurement are 3.453 MHz that used from 00:15 to 07:30 LT (UTC+7), and 7.102 MHz that used from 07:45 LT – 00:00 LT. The selection of those frequencies were also based on the legal permission to be use in the real world environment, as the author is member of amateur radio organization in Indonesia, namely ORARI.

3.3.3 Transmission Schedule and Measurement Timing

The measurement system is intended to be operated continuously and collect the result for a long period of measurement in the form of recording files. Therefore, the CIR measurement system needs to be set to work automatically and periodically for the effective and efficient of recorded file size. The CIR system is scheduled to work every 15 minutes for 24 hours a day with synchronization of sounding and recording time based on the internet reference time. However, due to the uncertainty of the time delay process from the SDR instrument (Ulversøy, 2010; Suksmono, 2013), a mismatch between the transmission and receiving time could occur. Therefore, to overcome this uncertainty of lag time, the scheduled time is added with time tolerance values both on the transmitter and receiver side. In the transmitter, the time for sounding the signal is set to start 3 seconds ahead of the recording signal in the receiver. On the receiver side, the recording time duration is extended three times from the sounding signal time duration in the transmitter. In practice, the scheduled transmission and receiving process is done using the Crontab-e functions that are already provided in UBUNTU operating system.

3.3.4 Link Budget Calculation

The output power of the transmission signal from HackRF one SDR device is only up to 0.03W (Great Scott Gadgets, 2021). To guarantee the transmitted signal could be arrived in the receiver antenna, the minimum required transmitted power could be calculated using equations as follows:

$$P_R = P_T + G_T + G_R + P_L \quad (6)$$

where P_R is the received Power (dBm), P_T is transmitted power (dBm), G_T is transmitted antenna gain (dBi), G_R is the received antenna gain (dBi), and P_L is the Path Loss (dB). For skywave propagation mode, P_L could be calculated using equation as follows:

$$P_L = L_a + L_{FSL} + L_g + L_p + L_q \quad (7)$$

where L_a is the absorption loss, L_g is ground loss, L_p is the polarization loss, L_q is the Loss from E layer, and L_{FSL} is the Free Space Loss. Regarding to McNamara (1991),

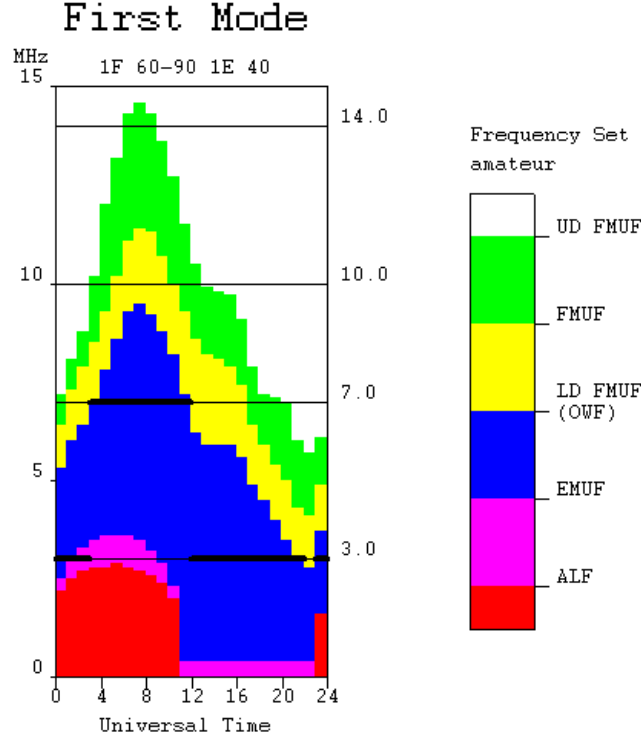


Figure 7. Result from ASAPS software for Bandung-Pameungpeuk circuits in December 2021. The selection of sounding frequency is based on the values between ALF and MUF

the maximum values of L_a , L_g , L_p , dan L_q is 20 dB, 3 dB, 6 dB and 9 dB, respectively. The value of L_{FSL} could be obtained using equation as follows:

$$L_{FSL} = 32,4 + 20\log(d) + 20\log(f) \quad (8)$$

where d is the distance of radio wave propagation path (km), and f is the frequency of radio wave (MHz). For NVIS propagation in this research, the distance (d) value is assumed to be 500 km and the frequency is 7 MHz. The distance value is obtained from two times values of average virtual height of F layer ($h'F$) which is 250 km. Using equation (8) and (9) the Path Loss value is 103,28 dB. For the minimum of required transmitted power, the minimum of P_R values could be based on the RTL-SDR receiver sensitivity which is -139 dBm (HB9JAG, 2013)). From equation (7) the minimum required of P_T is 4.2 mW to guarantee the signal will be received in the receiver. In this CIR measurement system, the modul of Radio Frequency Power Amplifier (RFPA) and Low Pass Filter (LPF) from commercial HF radio transmitter Icom IC-718 are used as shown in topside of Figure 8. The average output power from this module is up to 100 Watt for Amplitude Modulation and Single Side Band transmission (Icom Inc., 2015) which enough to be used in this system although some loss from cables and connector occurred. Together with the use of RFPA and LPF module in the transmitter site, the HF Broad band Folded Dipole Antenna is used for an effective signal transmission over the air. At the receiver site, the similar 30 meter long wire antenna is also use but with simpler receiver hardware device as shown in bottom side of Figure 8. The specification of the hardware that used in the CIR measurement system are described in Table 3.



Figure 8. Hardware device for transmitter site (topside) and receiver site (bottom side)

Table 3. Hardware Device and Specification of Ionosphere CIR measurement system

| Device | Transmitter | Receiver |
|--------------------|---|-------------------------------|
| SDR Hardware | HackRF One 20 Msps | RTL-SDR with HamitUp 3.2 Msps |
| SDR Software | GNU Radio 3.7 | GNU Radio 3.7 |
| Antenna | ICOM AH-710 (3-30 MHz) | ICOM AH-710 (3-30 MHz) |
| Personal Computer | Core i3 with UBUNTU 16.04 | Core i3 UBUNTU 18.06 |
| RF Power Amplifier | Icom IC-718 <i>Power</i> up to 100 Watt | none |

3.4 Data Post Processing

The recorded of the received signal $r(t)$ are in the form of complex values which could be written as follows:

$$rt = s(t) * h(t) \quad (9)$$

where $s(t)$ is the transmitted signal and $h(t)$ is the ionosphere channel impulse response. To obtain the ionosphere channel impulse response from the recorded signal, the cross-correlation calculation between $r(t)$ and $s(t)$ could be done using equation as follows:

$$h(\tau) = r_{sr}(\tau) = \int_{-\infty}^{\infty} s(t)r(\tau + t)\partial\tau \quad (10)$$

where $r_{sr}(\tau)$ is the cross-correlation between $s(t)$ and $r(t)$. According to (Sakar, 2003), the obtained of ionospheric channel impulse response are representing the Power Delay Profile (PDP) that can be written in equation (1). From Power Delay Profile, the calculation of the root mean square (r.m.s) of time delay or delay spread could be done using equation as follows:

$$\tau_{rms} = \sqrt{\frac{\sum_i |\alpha|^2 (\tau_i - (\frac{\sum_i |\alpha|^2 \tau_i}{\sum_i |\alpha|^2}))^2}{\sum_i |\alpha|^2}} \quad (11)$$

where τ_i is the time delay for each path i . For the calculation of the Doppler spread, equation (8) could be use to calculate the Doppler Spectrum $S(f)$ using equation as follows:

$$S(f) = \int_{-\infty}^{\infty} r_{hh}(\Delta t, \tau) e^{-j2\phi f \Delta t} \partial \Delta \tau \quad (12)$$

where r_{hh} is the autocorrelation of ionosphere channel impulse response. From the half of Doppler spectrum values, the Doppler spread could be determined.

4 Result From Operational Testing

An example result of the recorded received signal from single measurement is shown in Figure 9. This received signal will be used in the post-processing stage to obtain the ionosphere channel impulse response and its analysis. The received signal is shown in the form of time domain and frequency domain in the Intermediate Frequency (IF) spectrum. From the time-domain graph in Figure 9, the target of the received signal that will be used for the post-processing stage could not be seen clearly. However, in the frequency domain, the targeted of the received signal could be seen clearly which appears between 1 kHz to 3 kHz and starting from the second and ending at the fifth second of the recording time. The duration of the targeted received signal is matched with the duration of transmitted sounding signal as shown in Figure 4. From the received signal in Figure 9, it can be seen also that the receiver was able to receive another signal with different frequencies. During the measurement periods, some signals with significant power,

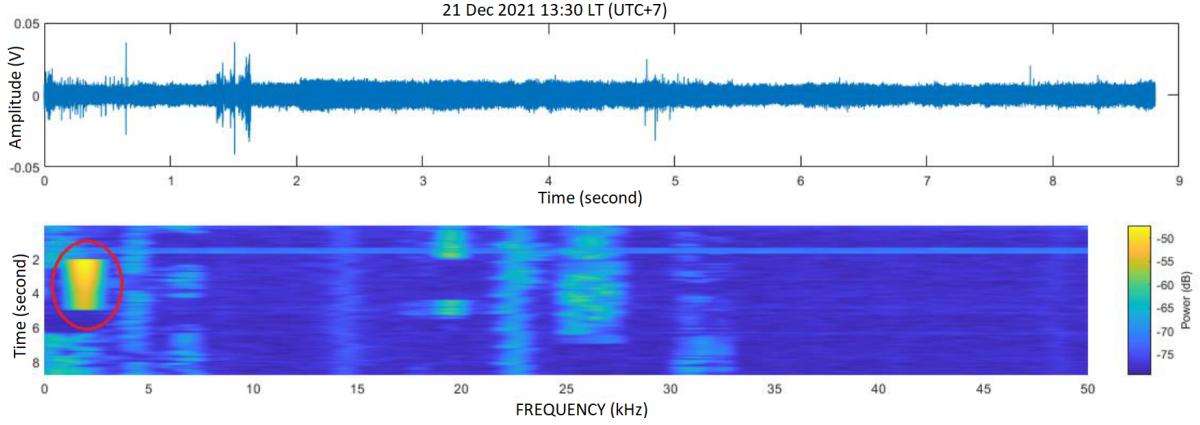


Figure 9. The received signal on 21 December 2021 at 13:30 LT (GMT+7). The targeted of the received sounding signal is between the 2nd and 5th second in the range of 1 kHz to 2.5 kHz at the Intermediate Frequency spectrum. The recorded signal also shows other received signals in different range of frequencies with significant power, bandwidth, and duration.

bandwidth, and durations in the frequencies 1 kHz, 4 kHz, 7 kHz, 15 kHz, 23 kHz, 26 kHz, and 32 kHz are also recorded. Those signals are representing another signal with different carrier frequency where its source could not be exactly identified as it could be from an amateur radio signal or broadcast station. In the range of the selected sounding frequency and in the transmission time period, it can be seen also there are some interference signals from the neighbour frequencies which could be influencing the post-processing of the received signal. From the Figure, it can be seen also that before the sounding signal was received, a wide band signal with a short period transmission time was received. This impulsive signal interference types is possible to be occurred in the same time of transmission sounding signal in the future and could not be avoided. Therefore, the redundancy technique by using 5 clusters of repeated PN bit sequences that are already explained in the methodology section is used for a mitigation.

From the received signal in Figure 9, the result of ionospheric channel impulse response calculation are shown in Figure 10. The observed of channel impulse response are consist of five cluster of Power Delay Profile with time different between the nearest neighbour cluster is around 0.4 second which follows the transmitted sounding signal as shown in Figure 4. From Figure 10b it can be seen the different number and magnitude of received impulse signal for each group. Those results show the system can captured the variation of the ionosphere channel in term of its propagation time delay. The smallest time delay that captured is 0.22 ms (CIR #1) and the highest time delay is 1.8 ms (CIR #3). Based on the specification of time delay resolution and the smallest value of delay spread given by ITU, the measurement system shows its capability to capture the ionosphere channel variation according to its specification designed. However, based on the values of the maximum of time delay that obtained in this result, the design of CIR systems could not confirm it's capabilities, yet. This condition could be occurred due to the quiet condition of ionosphere during the observation time. In Figure 11, ionogram from ionosonde during observation of CIR is shown to confirm the ionosphere conditions from its traces. It can be seen that the trace of the echo signal has clear and smooth shape without a small cusp or twist, and not spreading in time either in frequency which indicate the normal of ionosphere layers (Munro, 1953) (Munro and Heisler, 1958). From the confirmation of the quiet ionosphere condition in Figure 11, the maximum of time delay that obtained are reasonable and could be accepted.

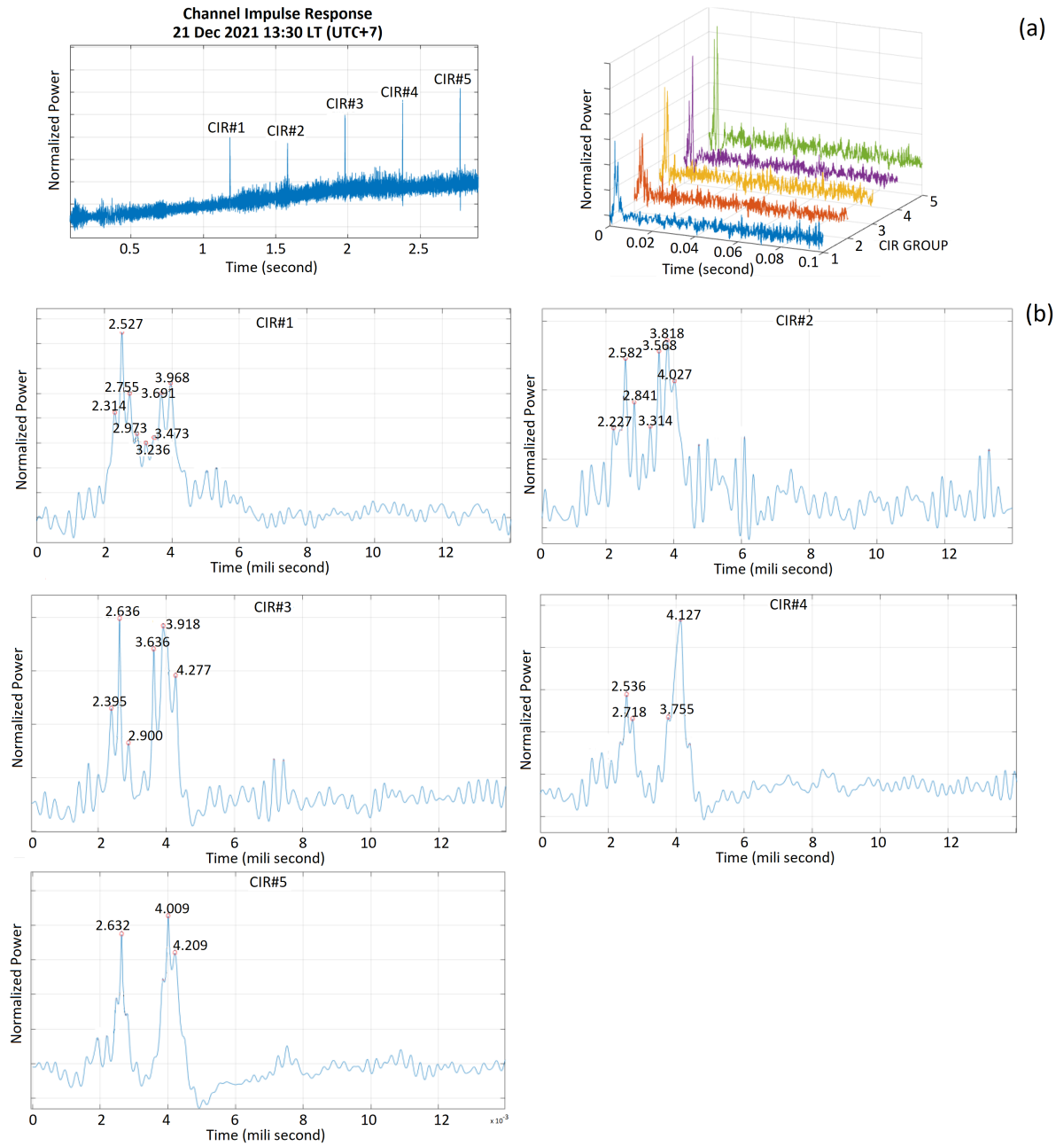


Figure 10. Ionospheric Channel Impulse Response result from 21st December 2021 at 13:30 LT (UTC+7). Five group of CIR was observed with two impulse cluster with different number and magnitude.

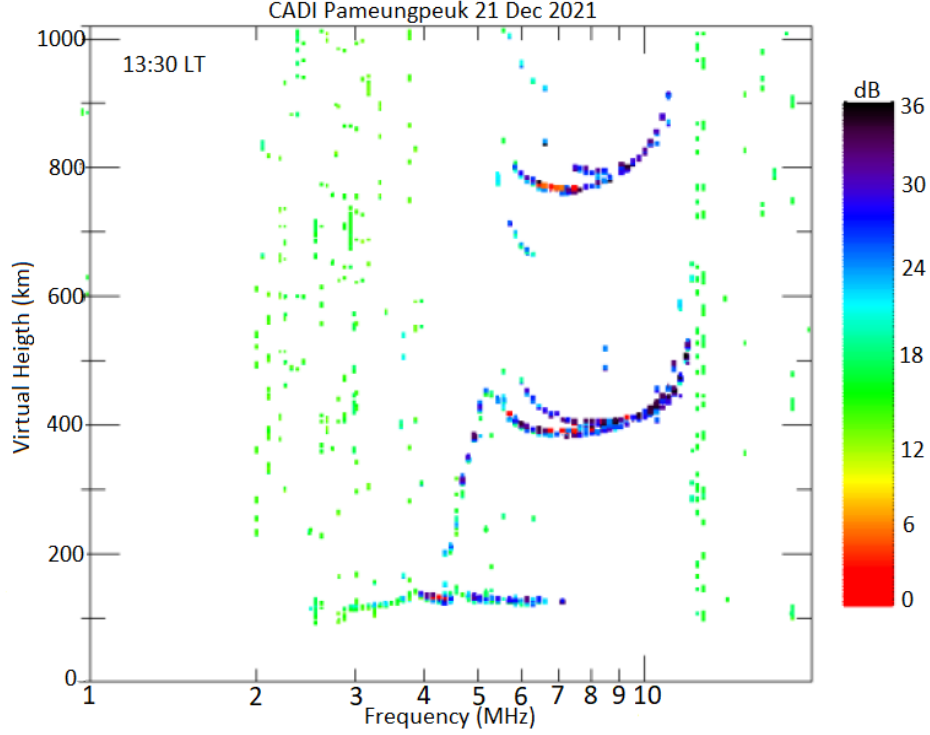


Figure 11. Ionogram from ionosonde at Pameungpeuk during the observation of CIR at 13:30 LT (UTC+7) on 21st December 2021 for the confirmation the stability and normal ionosphere conditions.

From ionogram in Figure 11, it can be seen also that E Sporadic layer were appeared with critical frequencies (f_oE_s) values more than 7 MHz where the CIR sounding frequency is used. The impact of the existence of E Sporadic layer was captured in the 5 group of CIR measurement result. In each of CIR group, we can see two cluster of impulse with variate amplitude (Figure 10). The presences of E Sporadic layer in the received impulse could be confirmed from its apparent distance calculation compared to the distance between virtual height of F layer and E layer. The different time between first impulse of second cluster and last impulse of first cluster in CIR #1 is $3.691 - 2.314 = 1.377$ ms. Therefore, the calculation of apparent distance travelling time between those two impulse clusters using speed of light c is 300000 km/s is 413.1 km. Half of this values is the estimation of different virtual height of E ($h'E$) and F ($h'F$) layers which is around 200 km. In this system, the absolute time delay that could be used for calculating the distance of the propagation path was not measured for the simplicity and the low cost of the designed system.

Early result measurement in the form of variation of Time Delay and Doppler frequency with their distributions from 15th December 2021 to 21st December 2022 are shown in Figure 12. Figure 12a show the root mean square (r.m.s) of time delay with its distribution. The r.m.s of time delay for 7 days observation is fluctuated with in range between 0 to 1,3 ms. This fluctuation show the ionosphere channel is change randomly. To obtained the general value of Delay spread, the statistical analysis approach of root mean square time delay could be done by using its distribution. From the distribution in Figure 12a, it can be seen that the mean of r.m.s delay spread is 4.627 ms and follows the Rayleigh distribution with the Delay spread values are tend to have more occurrence below its mean values. This one-week Delay Spread measurement values is different 0.373

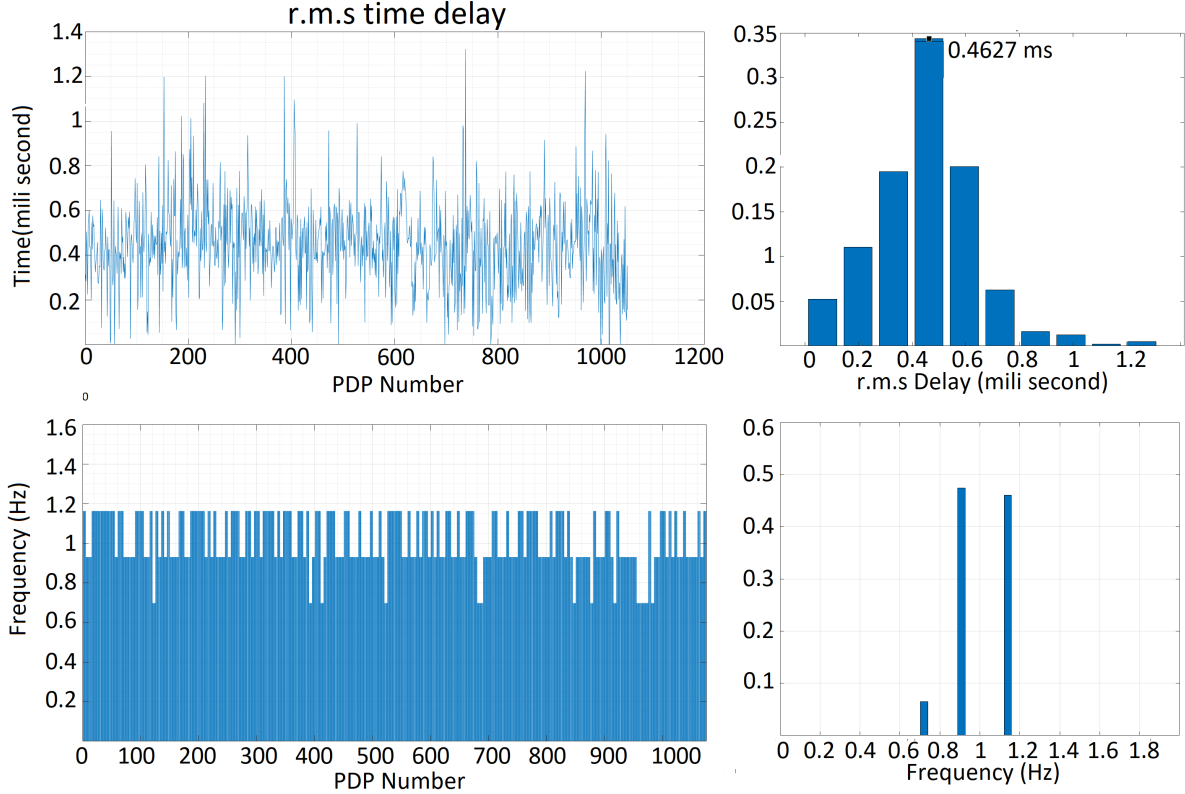


Figure 12. Result from one-day measurement for (a) Delay spread and (b) Doppler Spread

ms with recommendation values of Delay Spread ITU for low-latitude regions with normal ionosphere conditions. This difference value is affecting the determination of digital communication system parameters such as symbol period for an optimization. Therefore to have more accurate and detail values of Delay Spread, the measurement should be done for longer period. During the period of CIR measurement, ionosphere is in quiet condition based on the Kp and Dst index values which are between 0.6 to 3.6 (Matzka, 2022) and -12 to -31 (World Data Center et al., 2022), respectively.

Figure 12b shows the variation of Doppler spread with a range from 0.7 Hz to 1.1 Hz. The distribution of Doppler spread show the mean values is 0.9 Hz. Based on the Doppler spread that given by ITU, this value is higher 0.4 Hz from normal condition and lower 0.6 Hz for moderate condition in the low latitude region. This difference probably occurred due to the different mechanism of ionosphere formation in the EIA region from other low latitude region. The local ionosphere tilt in equator region could affecting the propagation of HF radio wave path as reported in (Maruyama et al, 2006). For validation, this value could be use to calculated the apparent velocity of ionosphere movement as the reflection object using equation $v = \frac{f_D}{f_c} c$ where f_D is the Doppler frequency and f_c is the sounding frequency. From equation (11) with f_D is 0.9 Hz and f_c is 7.12 MHz, the apparent velocity of ionosphere movement is 37.9 m/s. This value agreed with the result of vertical drift velocity of F layer ionosphere in equatorial region that done by (Namboothiri et al., 1989) which resulting the values between 10 ms to 40 ms. From early measurement result, it can be seen that the Ionosphere CIR measurement system is able to obtain the characteristic of the ionosphere channel in the form of Delay spread and Doppler spread parameters values. As the ionosphere follows the 11 years Solar cycle period as the longest temporal variation, the future result from long period of mea-

surement could be use for comprehensive ionosphere communication channel character-
istic.

5 Conclusion

The development of a channel impulse response measurement system over Java island, Indonesia for characterizing the Ionospheric communication channel in part of the Low latitude-Equatorial Ionosphere Anomaly (EIA) region was reported. The system resulting empirical data of Delay Spread and Doppler Spread parameter that could be used in designing the High-Frequency digital communication system. The specification of the measurement system was based on the increased value of ITU ionospheric channel recommendation in order to be able to capture the possibility of higher values that occurred in the EIA regions. From the early operating testing result, slightly different values of Delay Spread and Doppler Spread from ITU were found which probably due to the effect of EIA region. This measurement system is ready to be used for collecting more data in order to characterizing the Ionosphere communication channel over Java island Indonesia in comprehensively and also for investigation and dissemination of the space weather impact on the HF communication system.

Open Research Section

All data that used in this research are belongs to National Research and Innovation Agency and already stored in <https://zenodo.org/record/7552900> and <https://zenodo.org/record/7619093> with title Ionospheric Channel Impulse Response Measurement between Pameungpeuk and Bandung, Indonesia

Acknowledgments

We thanks to Dr. Rezy Pradipta from Boston College as a mentor in preparing the manuscript. We also thanks to technical team from Pameungpeuk and Bandung site for maintaining the operational of measurement system and for all technical support during campaign periods.

References

- Abadi, P., Otsuka, Y., and Tsugawa, T. (2015), Effects of pre-reversal enhancement of *EB* drift on the latitudinal extension of plasma bubble in Southeast Asia, *Earth, Planets and Space*, 67–74. <https://doi.org/10.1186/s40623-015-0246-7>.
- Abdu, M.A.,(2001), Outstanding problems in the equatorial ionosphere–thermosphere electrodynamics relevant to Spread-F, *Journal of Atmospheric and Solar-Terrestrial Physics*, Volume 63, Issue 9, 2001, PP: 869–884, ISSN 1364-6826, [https://doi.org/10.1016/S1364-6826\(00\)00201-7](https://doi.org/10.1016/S1364-6826(00)00201-7).
- Abdullah, S., Arief, A., and Muhammad, M., (2018). Utilization of NVIS HF Radio As Alternative Technologies In Rural Area of North Maluku. *Proceedings of the International Conference on Science and Technology, ICST*, pp. 734–39. doi: 10.2991/icst-18.2018.149.
- Ads, A. G., P. Bergadà, J. R. Regué, R. M. Alsina-Pagès, J. L. Pijoan, D. Altadill, D. Badia, and S. Graells. (2015), Vertical and Oblique Ionospheric Soundings over the Long Haul HF Link between Antarctica and Spain, *Radio Science*, 50(9):916–30. doi: 10.1002/2015RS005773.
- Andersen, J. B., Rappaport, T. S., and Yoshida, S., (1995) Propagation measurements and models for wireless communications channels, *IEEE Communications Magazine*, vol. 33, no. 1, pp. 42–49, Jan. 1995, doi: 10.1109/35.339880.
- Angling, J., Matthew, S., Paul Cannon, C., Nigel Davies, J. Tricia Willink, Vivianne Jodalen, and Bengt Lundborg. (1998), Measurements of Doppler and

- Multipath Spread on Oblique High-Latitude HF Paths and Their Use in Characterizing Data Modem Performance. *Radio Science*, 33(1):97–107.
- Bergadà, P., J. L. Pijoan, M. Salvador, J. R. Regué, D. Badia, and S. Graells. (2014), Digital Transmission Techniques for a Long Haul HF Link: DSSS versus OFDM, *Radio Science*, 518–30. doi: 10.1002/2013RS005203.1.
- Bole, A., Wall, A., and Norris A. (2014), Chapter 2 - The Radar System – Technical Principles, Radar and ARPA Manual (Third Edition), (Butterworth-Heinemann, PP: 29-137, ISBN 9780080977522, <https://doi.org/10.1016/B978-0-08-097752-2.00002-7>).
- Chen, G., Zhao, Z., Zhu, G., Huang, Y., and Li, T., (2010), HF Radio-Frequency Interference Mitigation, (*IEEE Geoscience and Remote Sensing Letters*, Vol. 7, no. 3, pp. 479-482, July 2010, doi: 10.1109/LGRS.2009.2039340).
- Commonwealth of Australia, Bureau of Meteorology, (2023), *ASAPS*. Retrieved from: <https://www.sws.bom.gov.au/ProductsandServices/1/2>
- Cox, Donald C. (1972) , Delay Doppler Characteristics of Multipath Propagation at 910 Mhz in a Suburban Mobile Radio Environment, *IEEE Transactions on Antennas and Propagation* 20(5):625–35. doi: 10.1109/TAP.1972.1140277.
- Davies, K. (1965), Ionospheric radio propagation (Vol. 80). *US Department of Commerce, National Bureau of Standards*.
- Drongowski (2020): *Ham It Up Upconverter*. Retrieve from: <https://support.nooelec.com/hc/en-us/articles/360005812474-Ham-It-Up-Upconverter>.
- Duncan, R., A. (1960), The equatorial F-region of the ionosphere, *Journal of Atmospheric and Terrestrial Physics*, Volume 18, Issues 2–3, 89-100, ISSN 0021-9169, [https://doi.org/10.1016/0021-9169\(60\)90081-7](https://doi.org/10.1016/0021-9169(60)90081-7).
- Eliardsson, P., Axell, E., Stenumgaard, P., Wiklundh, K., Johansson, B., and B. Asp (2015), Military HF communications considering unintentional platform-generated electromagnetic interference, *Proceeding 2015 International Conference on Military Communications and Information Systems (ICMCIS)*, 1-6, doi: 10.1109/ICMCIS.2015.7158700.
- Goodman (2005). The Ionosphere. In: Space Weather Telecommunications. *The International Series in Engineering and Computer Science*, vol 782. Springer, Boston, MA. <https://doi.org/10.1007/0-387-23671-63>
- Goldsmith, A (2005), Wireless Communications, *Cambridge University Press* p. 86, ISBN 978-0-521-83716-3
- Great Scott Gadgets (2021), *FAQ: What is the Transmit Power of HackRF?*. Retrieved from <https://hackrf.readthedocs.io/en/latest/faq.html>
- HB9JAG, (2013), *Some Measurements on DVB-T Dongles with E4000 and R820T Tuners: Image Rejection, Internal Signals, Sensitivity, Overload, 1dB Compression, Intermodulation*,. Retrieved from <https://www.rtl-sdr.com/measurements-on-rtl-sdr-e4000-and-r820t-dvb-t-dongles-image-rejection-internal-signals-sensitivity-overload-1db-compression-intermodulation/>
- Helmholtz Centre Potsdam German Research Centre for Geosciences GFZ (2023) (Kp-Index. Retrieved from: <https://kp.gfz-potsdam.de/en/data>
- Icom Inc.,(2015), *ICOM IC-718 Instruction Book*. Retrieved from <https://www.icomjapan.com/support/manual/1427/>
- International Telecommunication Union (2000), *Recommendation ITU-R Rec. F.1487. Testing of HF modems with bandwidths of up to about 12 kHz using ionospheric channel simulators*. Retrieved from <https://www.itu.int/rec/R-REC-F.1487-0-200005-I/en>
- Jiyo, (2013)., Analysis of Radio Wave Propagation Over Pameungpeuk-Bandung District Communication Circuit and Its Relations With Condition of Ionosphere, *Jurnal Sains Dirgantara*, Vol. 11, no. 1, pp. 29-40.
- Kitano, T.,Tomioka, Y., Subekti, A., Sadiq, M. A., Juzoji, H., and Nakajima, I.,(2006), A basic study of the near vertical inclined skywave the last sur-

- vival tool of radio communications to support telemedicine after n-disaster, *HEALTHCOM 2006 8th International Conference on e-Health Networking, Applications and Services*, pp. 165-169, doi: 10.1109/HEALTH.2006.246440
- Kurniawati, I, Hendranto, G., and Taufik M, (2018) Statistical Modeling of Low-Latitude Long-Distance HF Ionospheric Multi-Mode Channels. *Progress in Electromagnetic Research Vol. 64*, PP:77–86. doi: 10.2528/PIERM17101603.
- Laufer, C., (2014), *The Hobbyist's Guide to the RTL-SDR: Really Cheap Software Defined Radio*: Kindle Edition. RTL-SDR.com
- Maruyama, T. and Kawamura, M. (2006), Equatorial ionospheric disturbance observed through a transequatorial HF propagation experiment, *Ann. Geophys.*, 24, 1401–1409, <https://doi.org/10.5194/angeo-24-1401-2006>.
- Maslin, N.M. (1988), *HF Communications: A Systems Approach* (1st ed.). *CRC Press.*, <https://doi.org/10.4324/9780203168899>
- Matzka, Jürgen; Bronkalla, Oliver; Tornow, Katrin; Elger, Kirsten; Stolle, Claudia (2021): Geomagnetic Kp index. V. 1.0. GFZ Data Services. <https://doi.org/10.5880/Kp.0001>
- McNamara, L., F., (1991), *The Ionosphere: Communications, Surveillance, and Direction Finding*, *Kruger Pub. Co.*, Malabar, 1991.
- Murugan, M., Purandare R., G., and Tavildar A., S., (2008), Near Vertical Incidence Skywave (NVIS) Propagation. *Proceedings of the international conference on sensors, signal processing, communication, control and instrumentation (SSPCCIN) January 3-5, VIT Pune, India*
- Munro, G. H. (1953). Reflexions from irregularities in the ionosphere. *Proceedings of the Royal Society of London A*, 219, 447–463.
- Munro, G. H., Heisler, L. H. (1958). Ionospheric records of solar eclipses. *Journal of Atmospheric and Solar-Terrestrial Physics*, 12, 57–67.
- Namboothiri, S. P., Balan, N., and Rao, P. B. (1989), Vertical plasma drifts in the F region at the magnetic equator, *J. Geophys. Res.*, 94(A9), 12055– 12060, doi:10.1029/JA094iA09p12055.
- Ossmann, M., (2016), *Software defined radio with HackRF*. Retrieved from: <https://greatscottgadgets.com/sdr>
- Pirkl, Ryan J., and Gregory D. Durgin. (2008), Optimal Sliding Correlator Channel Sounder Design, *IEEE Transactions on Wireless Communications* 7(9):3488–97. doi: 10.1109/TWC.2008.070278.
- Porte, J., Maso, J. Pijoan, J., Miret, M., Badia, D., and Jayasinghe, J., (2018) Education and e-health for developing countries using NVIS communications, *2018 IEEE Region 10 Humanitarian Technology Conference (R10-HTC)*, pp. 1-5, doi: 10.1109/R10-HTC.2018.8629842.
- Salous, S., (2013), *Radio Propagation Measurement and Channel Modelling*, 1st ed., Wiley, 2013, pp.182-191.
- Suksmono, A., B., (2013), A Simple Solution to the Uncertain Delay Problem in USRP Based SDR-Radar Systems, *arXiv* 1309.4843, pp. 1-4, 2013
- Ulverson, T., (2010), Software Defined Radio: Challenges and Opportunities, *IEEE Communications Surveys Tutorials*, vol. 12, no. 4, pp. 531-550, Fourth Quarter 2010, doi: 10.1109/SURV.2010.032910.00019.
- Wang, J., Ding, G., and Wang, H. (2018). HF Communications: Past, Present, and Future. *China Communications*, 15, 1–9
- Withington, T. (2020, June 10). *HF Radio: Still Valid After 100 Years*. Retrieved from <https://www.asianmilitaryreview.com/2020/06/hf-radio-still-valid-after-100-years>
- World Data Center for Geomagnetism, Kyoto, M. Nose, T. Iyemori, M. Sugiura, T. Kamei (2015), Geomagnetic Dst index, doi:10.17593/14515-74000